

# Evidence of fast rotation in dwarf elliptical galaxies

S. Pedraz,<sup>1,2\*</sup> J. Gorgas,<sup>1</sup> N. Cardiel,<sup>1</sup> P. Sánchez-Blázquez<sup>1</sup> and R. Guzmán<sup>3</sup>

<sup>1</sup>*Departamento de Astrofísica, Facultad de Ciencias Físicas, Universidad Complutense de Madrid, E28040-Madrid, Spain*

<sup>2</sup>*Calar Alto Observatory, CAHA, Apdo. 511, 04004 Almería, Spain*

<sup>3</sup>*Department of Astronomy, University of Florida, P.O. Box 112055, Gainesville, FL 32611-2055*

Accepted 2002 April 9. Received 2002 April 1; in original form 2001 December 20

## ABSTRACT

In this Paper we investigate the kinematical properties of early-type dwarfs by significantly enlarging the scarce observational sample so far available. We present rotation curves and mean velocity dispersions for four bright dwarf ellipticals and two dwarf lenticular galaxies in the Virgo cluster. Most of these galaxies exhibit conspicuous rotation curves. In particular, five out of the six new galaxies are found to be close to the predictions for oblate spheroids flattened by rotation. Therefore, and contrary to the previous observational hints, the present data suggest that an important fraction of dwarf early-type galaxies may be rotationally supported.

**Key words:** galaxies: dwarf – galaxies: elliptical and lenticular, cD – galaxies: kinematics and dynamics

## 1 INTRODUCTION

Although dwarf elliptical galaxies (dEs) constitute the dominant galaxy population in nearby clusters, their origin and nature are still unclear. One of the main questions under debate is whether dEs represent the extension of the “classical” ellipticals (Es) to lower luminosities, or, on the contrary, whether they are the result of distinct formation and evolution processes (for a review see, e.g., Ferguson & Binggeli 1994). While early observational works suggested a dichotomy in the structural properties of both galaxy families (e.g. Kormendy 1985), Binggeli & Jerjen (1998) (see also Jerjen & Binggeli 1997) have shown that, if a Sérsic law is used to fit the observed luminosity profiles, dEs appear as the true low-luminosity extension of the classical Es. Previous workers have also studied the possible dichotomy between dEs and Es by comparing the flattening distributions (e.g. Ryden & Terndrup 1994), clustering properties (Conselice, Gallagher & Wyse 2001) and stellar populations (Gorgas et al. 1997, hereafter G97; Drinkwater et al. 2001) of dEs in nearby clusters. Another key issue that should provide important clues to the open question of the possible dichotomy is the analysis of rotational properties.

From the work of Davies et al. (1983) (see also Halliday et al. 2001), it is well known that low-luminosity E galaxies, in contrast with giant Es, are supported by rotation. If dEs were the extension to even lower luminosities of the classical Es, one should expect to find relatively high rotational velocities along the major axis of these objects. The observational data in this subject require high signal-to-noise

(S/N) spectra at faint levels of surface brightnesses and it is, therefore, very scarce. Until recently, rotation curves had only been measured for 6 dEs: two dwarfs in Virgo (VCC 351 and IC 794; Bender & Nieto 1990, hereafter BN90), the 3 dwarfs companions of M31 (e.g. Bender, Paquet & Nieto 1991) and the Fornax dE (Mateo et al. 1991). In all these cases, dEs were found to rotate too slowly to be consistent with an oblate, isotropic body flattened by rotation. Very recently, new data have been added to this sparse statistics. On the one hand, Geha, Guhathakurta & van der Marel (2001, hereafter GGV01) have presented kinematical data for a sample of 4 Virgo dEs, finding that, in agreement with the previous results, they are slow rotators. On the other hand, De Ricke et al. (2001, hereafter DR01) have obtained deep spectroscopic data of the dE FS76 (in the NGC 5044 group), showing that the galaxy is rotating as fast as predicted by the isotropic models. In this Paper we revisit the question of rotation in dEs by practically doubling the observational sample so far available. We will show that most of the galaxies in the new sample tend to be rotationally supported and, therefore, fast rotation in dwarf elliptical galaxies is not a rare event, as previously thought.

## 2 GALAXY SAMPLE, OBSERVATIONS AND DATA REDUCTION

The galaxies analysed in this work correspond to those already presented in G97. This sample of Virgo galaxies, which is listed in Table 1, comprises 4 dwarf ellipticals and two dwarf lenticular galaxies. Although NGC 4489 is classified as S0 (non dwarf) in Binggeli, Sandage & Tammann (1985),

\* E-mail: spm@astrax.fis.ucm.es

**Table 1.** Kinematic data for the galaxy sample. Galaxy types have been taken from Binggeli, Sandage & Tammann (1985). Absolute magnitudes have been computed using a distance modulus to Virgo of  $-30.82$ , which corresponds to  $H_0 = 75 \text{ km s}^{-1} \text{ Mpc}^{-1}$ . PA is the slit position angle (north to east), which corresponds to the major axis position according to the following references: (1) Jedrzejewski (1987); (2) Paturel et al. (1989), and (3) Binggeli & Cameron (1993). Sources for ellipticities ( $\epsilon$ ) are: (3) Binggeli & Cameron (1993); (4) Mean from Binggeli et al. (1985) and Djorgovski (1985); (5) Ryden et al. (1999), and (6) GGV01. The central velocity dispersions ( $\sigma_0$ , in  $\text{km s}^{-1}$ ) correspond to a  $2'' \times 4''$  central aperture. Mean velocity dispersions ( $\bar{\sigma}$ ), maximum rotational velocities ( $V_{\text{max}}$ ) and the anisotropy parameters ( $(V/\sigma)^*$ ), together with their formal errors, have been derived as explained in the text.

Galaxy	Type	$M_B$	PA	Source	$\epsilon$	Source	$\sigma_0$	$\bar{\sigma}$	$V_{\text{max}}$	$(V/\sigma)^*$
NGC 4415	dE1,N	-17.10	0	2	0.11	3	$42.7 \pm 4.2$	$41.7 \pm 2.2$	$20.9 \pm 1.2$	$1.43 \pm 0.38$
NGC 4431	dS0(5),N	-17.12	177	2	0.42	5	$41.9 \pm 4.9$	$52.9 \pm 2.1$	$32.0 \pm 6.3$	$0.71 \pm 0.16$
NGC 4489	S0 <sub>1</sub> (1)	-17.98	160	1	0.08	4	$51.1 \pm 1.8$	$50.3 \pm 1.4$	$22.8 \pm 8.1$	$1.55 \pm 0.73$
IC 794	dE3,N	-16.62	110	2	0.24	6	$41.1 \pm 3.2$	$43.4 \pm 2.5$	$3.4 \pm 1.7$	$0.14 \pm 0.07$
IC 3393	dE7,N	-16.07	133	3	0.52	5	$25.0 \pm 7.6$	$26.8 \pm 4.3$	$18.0 \pm 1.7$	$0.65 \pm 0.14$
UGC 7436	dE5	-16.02	120	2	0.44	5	$35.0 \pm 4.1$	$36.7 \pm 2.8$	$14.9 \pm 3.1$	$0.47 \pm 0.11$

it exhibits a mean surface brightness within the effective radius of  $SB_e = 22.24 \text{ mag arcsec}^{-2}$  (Faber et al. 1989), which, in the  $SB_e$ -absolute magnitude plane, places it closer to the locus of dwarf ellipticals than to the low-luminosity early-type galaxies<sup>1</sup>. It must be noted also that the present sample is biased toward the brightest dwarf early-type galaxies of the Virgo cluster.

Long-slit spectroscopic observations along the major axes of the galaxies were carried out with the INT at La Palma. Although the relevant observational parameters were already described in G97, we want to highlight that high-quality spectra, covering the 4700–6100 Å range with a spectral resolution of  $\sigma = 60 \text{ km s}^{-1}$  (FWHM  $\sim 2.5 \text{ \AA}$ ) were obtained out to, typically, the effective radii of the galaxies.

The data reduction and analysis were performed using the `REDUCE` package (Cardiel et al. 1998; Cardiel 1999), specially developed for the parallel treatment of data and errors in the reduction of spectroscopic observations. In this sense, each fully processed spectrum is accompanied by an associated error spectrum, which contains the propagation of the initial random errors (due to photon statistics and read-out noise) throughout the cascade of arithmetic manipulations in the reduction procedure. Full details concerning the data reduction will be presented in Pedraz (2002).

We complemented the observations of the targets with a large set (39) of template stars from the Lick/IDS stellar library (Gorgas et al. 1993; Worthey et al. 1994). The template list was selected to provide an appropriate coverage in stellar atmospheric parameters ( $T_{\text{eff}}$  from 3247 to 6575 K,  $\log g$  from 1.11 to 4.84, and  $[\text{Fe}/\text{H}]$  from  $-2.15$  to 0.35), suitable for the modelling of old stellar populations.

### 3 MEASUREMENT OF KINEMATIC DATA

In order to estimate radial velocities and velocity dispersions for each galaxy spectrum, we wrote a dedicated program within `REDUCE` which follows the `MOVE` and `OPTEMA` algorithms described by González (1993). The `MOVE` algorithm, an improvement of the classic Fourier quotient

<sup>1</sup> At the absolute magnitude of NGC 4489, classical ellipticals and S0's attain typical values of  $SB_e$  between 18 and 21  $\text{mag arcsec}^{-2}$ , whereas for the dwarf galaxies of this sample  $22.5 < SB_e < 23 \text{ mag arcsec}^{-2}$ .

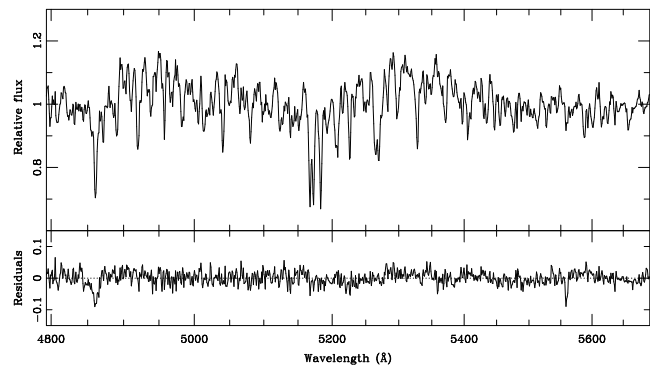


**Figure 1.** Upper panel: Central spectrum of NGC 4415. The spectrum has been continuum subtracted and normalized. Bottom panel: Residuals of the galaxy-composite template fit, corresponding to the computed kinematic parameters ( $\gamma = 0.814$ ,  $V_0 = 926.5 \text{ km s}^{-1}$  and  $\sigma = 42.7 \text{ km s}^{-1}$ ). The scale is the same than in the upper plot.

method by Sargent et al. (1977), is an iterative procedure in which a galaxy model is processed in parallel to the galaxy spectrum. In this way, a comparison between the input and recovered broadening functions for the model allows to correct the galaxy power spectrum from any imperfections of the data handling in Fourier space. The main improvement of the procedure is introduced through the `OPTEMA` algorithm, which is able to overcome the typical template mismatch problem. First, the 39 individual stellar spectra of the observing run were binned to create a set of 8 template spectra corresponding to different spectral types and luminosity classes (namely F0V, G0V, K0V, M0V, G5III, G8III, K0III, K5III). For each galaxy central spectrum, these 8 template spectra are scaled, shifted and broadened according to a first guess of the  $\gamma$  (mean line strength),  $V$  (radial velocity) and  $\sigma$  (velocity dispersion) parameters. The next step is to find the linear combination of the template spectra that best matches the observed galaxy spectrum. This provides a first composite template which is fed to the `MOVE` algorithm. The output kinematic parameters are then used to create an improved composite template and the process is iterated until it converges. This iterative approach then provides an optimal template while simultaneously computing the radial velocity and velocity dispersion of the galaxy spectrum. In Figure 1 we show a typical fit between the central spectrum

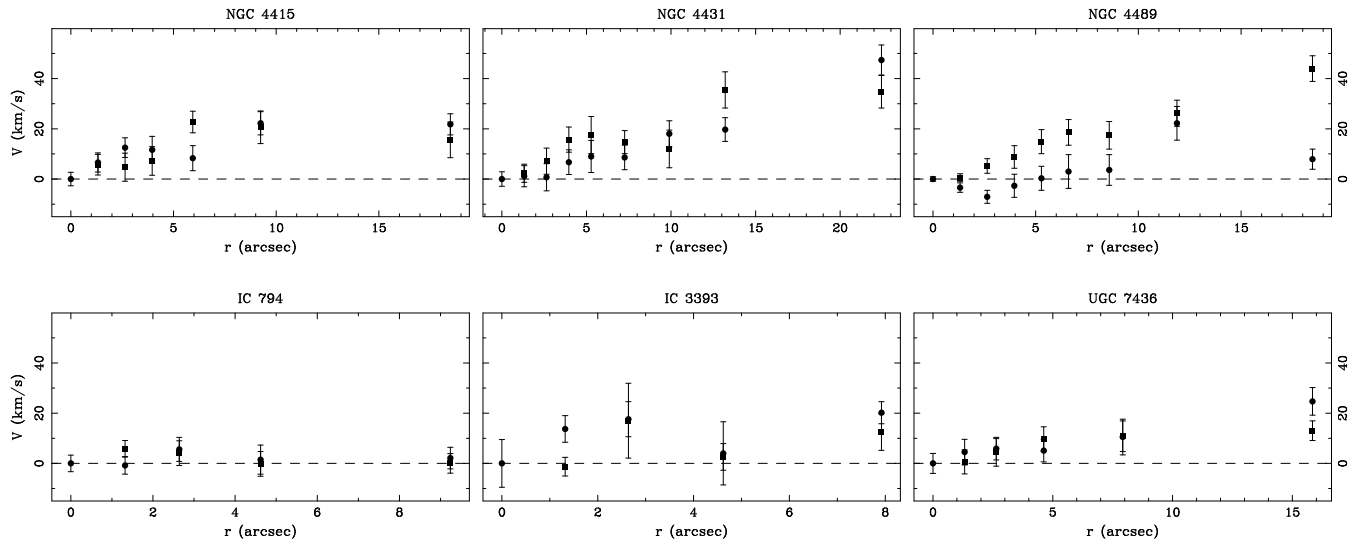


**Figure 2.** Rotational velocities  $V$  against radius  $r$  in arc seconds for the galaxy sample ( $1''$  corresponds to  $\sim 71$  pc). The profiles are folded around the center, with circles and squares corresponding to different galaxy sides.

of a galaxy of the sample and its corresponding optimal template corrected with the derived kinematic parameters. It must be noted that, once an optimal template is derived for the central spectrum of a given galaxy, this same template is used to derive the kinematics of the different spectra along the galaxy radius. This is a fair approximation since these galaxies exhibit relatively flat stellar population gradients along the radius (G97).

For each galaxy spectrum, random errors in the derived kinematic parameters were computed by numerical simulations. In each simulation, a bootstrapped galaxy spectrum, computed from the error spectra provided by the reduction with REDUCE by assuming Gaussian errors, is fed to the algorithms described above (note that a different optimal template is computed in each simulation). Errors in the parameters are then calculated as the unbiased standard deviations of the different solutions. These final errors are expected to be quite realistic, since they incorporate all the uncertainties of the whole reduction process, from the first reduction steps (e.g. flatfielding) to the final measurements of the kinematics.

In order to assess the sensitivity of the above fitting procedure to measure velocity dispersions of only a fraction of the spectral resolution ( $\sigma_{\text{instr}}$ ), we carried out several Monte Carlo simulations in which we added Gaussian noise to artificially broadened stars. To summarize, we conclude that, in order to measure a velocity dispersion of  $\sigma_{\text{instr}}/2$  (30 km/s for our instrumental setup) with a relative error below 50% ( $< 15$  km/s) we needed galaxy spectra with a minimum S/N (per  $\text{\AA}$ ) of 20–25.

Central velocity dispersions  $\sigma_0$ , together with their corresponding random errors, for the galaxy sample are listed in Table 1. We must note that S/N for the central spectra ranged from 38 to 98. The central velocity dispersion of NGC 4489 has been already measured by several authors. Our result ( $\sigma_0 = 51.1 \pm 1.8$ ) agrees with some of the previous measurements, like those of Davies et al. (1983;  $\sigma_0 = 53 \pm 15$ ), Faber et al. (1989;  $\sigma_0 = 49 \pm 7$ ) and González (1993;  $\sigma_0 = 48 \pm 3$ ), but it is somewhat smaller than the

values given by Simien & Prugniel (1997;  $\sigma_0 = 63 \pm 13$ ) and, especially, Smith et al. (2000;  $\sigma_0 = 72 \pm 7$ ). We must note that the spectral resolution of these two last works ( $\sigma_{\text{inst}} \approx 100 \text{ km s}^{-1}$ ) is dangerously high to derive accurate velocity dispersions at these levels. IC 794 has also been included in previous kinematics works. Our central velocity dispersion ( $\sigma_0 = 41.1 \pm 3.2$ ) is marginally smaller than the value obtained by BN90 ( $\sigma_0 = 52 \pm 6$ ) but it perfectly agrees with the recent result of GGV01 ( $\sigma_0 = 41.6 \pm 0.9$ )<sup>2</sup>. Central velocity dispersions for NGC 4431, IC 3393 and UGC 7436 have already been listed in the compilation by Bender et al. (1992). We must note that these values (68, 55 and 45 km/s respectively) are significantly larger than our measurements (42, 25 and 35 km/s). The original source of those values is unpublished data from R. Bender and, therefore, we do not have information enough to untangle the origin of this discrepancy. In any case, given the high S/N ratios of our spectra and the comparison with the previous published works, we are confident that our velocity dispersions are free of significant biases.

Folded rotation velocity curves along the major axes of the galaxies are presented in Figure 2. For the outer regions, we co-added a sufficient number of spectra in the spatial direction to guarantee a minimum signal-to-noise per  $\text{\AA}$  of 20. In the case of NGC 4415, NGC 4431 and UGC 7436 the profiles extend out to the effective radius of the galaxies, whereas, for the other three galaxies, the data reach roughly to half the effective radius. The quality of the data and reliability of the error bars is apparent by the typical agreement between symmetrical points at both galaxy sides. An exception is the rotation curve for NGC 4489. In this case, a displacement of 1.3 arcsec in the kinematic centre can explain the asymmetry.

<sup>2</sup> This value has been computed, after the digitization of Fig. 1 in GGV01, as the error weighted mean of all the measurements with  $r < 2''$ .

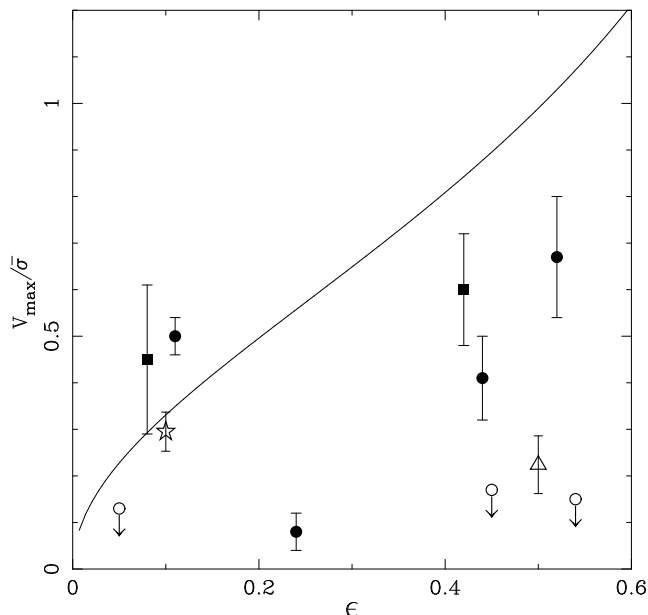


**Figure 3.** Ratio of maximum rotational velocity to mean velocity dispersion versus galaxy ellipticity. Filled points are the data from this paper (circles: dEs; squares: dS0s). Open circles, the triangle and the star show respectively data from GGV01, BN90 and DR01. The line represents the prediction for isotropic oblate galaxies flattened by rotation from Binney (1978).

#### 4 DISCUSSION

In order to quantify the rotational support of the objects we follow the usual procedure of comparing the maximum rotational velocity ( $V_{\max}$ ) to the mean velocity dispersion ( $\bar{\sigma}$ ). A conservative estimate of the parameter  $V_{\max}$  was computed as the error-weighted mean of the two data pairs with the highest rotational velocities. In some galaxies, like NGC 4431 and UGC 7436, the rotation curves increase to the outermost points observed, so the derived  $V_{\max}$  should be considered as lower limits to the actual values. To compute the mean velocity dispersion we coadded all the individual spectra with radii between  $1''$  and the effective radius. Prior to this, we shifted all the spectra to the same wavelength scale by using the rotation curves displayed in Fig 2. The resulting spectra exhibit S/N ratios, per  $\text{\AA}$ , ranging from 62 to 119. Final values of  $V_{\max}$  and  $\bar{\sigma}$ , together with their corresponding errors, are listed in Table 1.

In Figure 3 we have plotted the ratio  $V_{\max}/\bar{\sigma}$  against mean ellipticity (compiled from the most recent available estimates in the literature – see caption to Table 1). The previous measurements from BN90 (for VCC 351), GGV01 (for VCC 917, VCC 1254 and VCC 1876) and DR01 (for FS 76) are also included. For IC 794, also in the samples of BN90 and GGV01, we only plot the ratio computed in this work. However, it is important to note that our estimate for this galaxy ( $V_{\max}/\bar{\sigma} = 0.08 \pm 0.04$ ) is in perfect agreement with the upper limits given by the previous works ( $< 0.20$  in BN90, and  $< 0.12$  in GGV01). This gives further support to the data presented in this paper. We must also note that, to be fully consistent, we have recalculated the  $V_{\max}/\bar{\sigma}$  ratio for the galaxy in DR01 using the same procedure than for our sample (DR01 give a ratio of peak velocity to central velocity

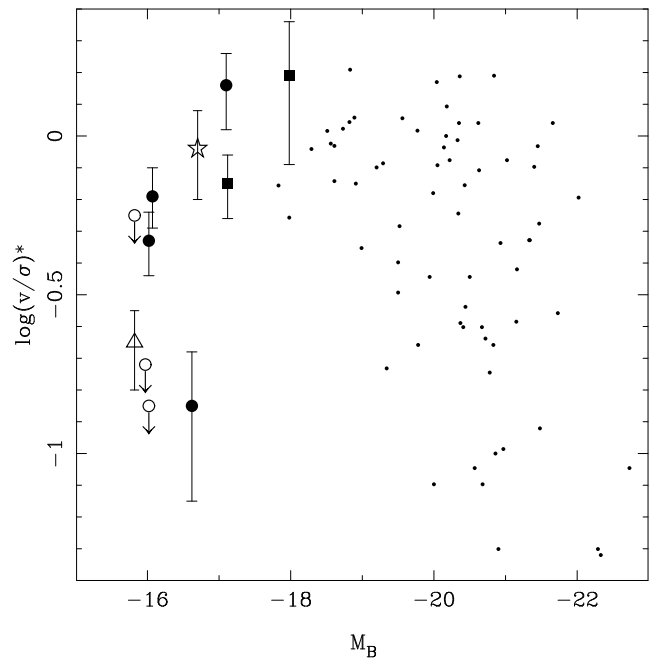


**Figure 4.** Logarithm of the anisotropy parameter (ratio of the observed value of  $V_{\max}/\bar{\sigma}$  to the one predicted by the isotropic model) against absolute magnitude. Small points show the data from Bender, Burstein & Faber (1992) for giant and intermediate ellipticals corrected to  $H_0 = 75 \text{ km s}^{-1} \text{ Mpc}^{-1}$ . The rest of the symbols are the same as in Figure 3.

dispersion of  $0.33 \pm 0.15$ ). After digitizing the measurements in their Fig. 2, we obtain a ratio of  $0.30 \pm 0.04$ .

The curve in Figure 3 shows the expected relationship for an oblate spheroid with isotropic velocity distribution, thus rotationally flattened, from Binney (1978). As it is apparent from this figure, while the dwarf galaxies included in the previous works (with the exception of DR01) were found to rotate too slowly to be consistent with the isotropic model, 5 out of the 6 dwarf early-type galaxies studied in this paper (and 3 out of the 4 dEs) are compatible with being rotationally supported. We recall that the rotational velocities for the two galaxies at  $\epsilon \sim 0.4$  could be in fact lower limits of their actual values.

To investigate this issue in more detail, in Figure 4 we present a plot of the anisotropy parameter (ratio of the observed value of  $V_{\max}/\bar{\sigma}$  to the one predicted by the isotropic model) against absolute magnitude. In order to compare the properties of dEs with those of giant and low-luminosity Es, we have included the galaxies from the compilation of Bender, Burstein & Faber (1992). Concerning the three galaxies in common with their sample (NGC 4431, IC 3393 and UGC 7436; see above), we must note that their  $V_{\max}/\bar{\sigma}$  values (1.00, 0.50 and 0.44, respectively) are not incompatible with ours ( $0.71 \pm 0.16$ ,  $0.65 \pm 0.14$ ,  $0.47 \pm 0.11$ ).

In their study of the fundamental plane, Bender et al. (1992) (see also BN90) noted that galaxies with anisotropic velocity distributions were found at both high and low values of mass. Apart from confirming these findings, the new results presented in Figure 4 show that the brightest early-type dwarfs of the sample tend to be rotationally supported, extending the behaviour of the low-luminosity ellipticals towards the bright end of the dwarf family. Furthermore, these

data indicate that, for fainter luminosities ( $M_B \geq -17$ ), and as it was the case for the bright ellipticals, dwarf galaxies exhibit a range of rotational properties (i.e. not all dEs are supported by anisotropy).

In spite of these results, the present sample is still too small to derive firm conclusions about the possible relation between rotational support and other parameters. For instance, there are nucleated and non-nucleated dwarfs among both the rotating and non-rotating subsamples. Note that the search for correlations between rotational support and other properties is essential to test the possible existence of a dichotomy within the dE family (as suggested by Ryden et al. 1999) similar to that found for the Es (in isophote shapes, rotation, and core properties).

It is also specially interesting to compare the rotational properties with the stellar population of dEs. We must highlight that, with the exception of NGC 4489 (a possible transition object between dS0 and S0), the only galaxy of our sample flattened by anisotropic velocity dispersion (IC 794) is clearly the most metal-rich and youngest object in G97 (see their Figure 1.b). If confirmed by additional stellar populations measurements of other non-rotating dEs, this still speculative result would give support to a scenario in which recent star formation episodes are linked to a decrease in rotational support. In this sense, this would agree with the suggestion by BN90 that supernova-driven winds, triggered by star formation, could cause anisotropic supported objects. Also, both low rotation and young stellar populations are simultaneously predicted by the harassment models of Moore, Lake and Katz (1998), in which cluster dE are the result of morphological transformation of accreted spiral galaxies. This tentative correlation between rotation and age is in the opposite sense to that found for classical ellipticals, in which fast-rotating Es tend to have disk-like isophotes and younger ages (Bender 1988; de Jong & Davies 1997).

In any case, and independently of the possible link between rotation and star formation, the present results are compatible with the diversity of rotational properties predicted by the harassment scenario (compare our Fig. 4 with Fig. 7 of Moore et al. 1998). More data is clearly needed to understand the driving parameters governing the dynamical properties of dEs, as well as the possible correlation of rotation with luminosity profiles, isophotal shapes, core properties (nucleated versus non-nucleated) and stellar populations.

## ACKNOWLEDGMENTS

The INT is operated on the island of La Palma by the Royal Greenwich Observatory at the Observatorio del Roque de los Muchachos of the Instituto de Astrofísica de Canarias. This work was supported in part by the Spanish Programa Nacional de Astronomía y Astrofísica under grant AYA2000-977.

## REFERENCES

Bender R., 1988, *A&A*, 193, L7  
 Bender R., Nieto J.-L., 1990, *A&A*, 239, 97 (BN90)  
 Bender R., Paquet A., Nieto J.-L., 1991, *A&A*, 246, 349  
 Bender R., Burstein D., Faber S.M., 1992, *ApJ*, 399, 462

Binggeli B., Cameron L.M., 1993, *A&AS*, 98, 297  
 Binggeli B., Jerjen H., 1998, *A&A*, 333, 17  
 Binggeli B., Sandage A., Tammann G.A., 1985, *AJ*, 90, 1681  
 Binney J., 1978, *MNRAS*, 183, 501  
 Cardiel N., 1999, Ph.D. thesis, Universidad Complutense de Madrid  
 Cardiel N., Gorgas J., Cenarro J., González J.J., 1998, *A&A*, 127, 597  
 Conselice C.J., Gallagher J.S. III, Wyse R.F.G., 2001, *ApJ*, 559, 791  
 Davies R.L., Efstathiou G., Fall S.M., Illingworth G., Schechter P.L., 1983, *ApJ*, 266, 41  
 De Jong R.S., Davies R.L., 1997, *MNRAS*, 285, L1  
 De Rijcke S., Dejonghe H., Zeilinger W.W., Hau G.K.T., 2001, *ApJ*, 559, L21 (DR01)  
 Djorgovski S., 1985, Ph.D. thesis, University of California, Berkeley  
 Drinkwater M.J., Gregg M.D., Holman B.A., Brown M.J.I., 2001, *MNRAS*, 326, 1076  
 Faber S.M., Wegner G., Burstein D., Davies R.L., Dressler A., Lynden-Bell D., Terlevich R.J., 1989, *ApJS*, 69, 763  
 Ferguson H.C., Binggeli B., 1994, *A&A Rev.*, 6, 67  
 Geha M., Guhathakurta P., van der Marel R., 2001, in Natarajan P., ed., *The Shapes of Galaxies and their Halos*, in press (astro-ph/0107010) (GGV01)  
 González J.J., 1993, Ph.D. thesis, University of California, Santa Cruz  
 Gorgas J., Faber S.M., Burstein D., González J.J., Courteau S., Prosser C., 1993, *ApJS*, 86, 153  
 Gorgas J., Pedraz S., Guzmán R., Cardiel N., González J.J., 1997, *ApJ*, 481, L19 (G97)  
 Halliday C., Davies R.L., Kuntschner H., Birkinshaw M., Bender R., Saglia R.P., Baggle G., 2001, *MNRAS*, 326, 473  
 Jedrzejewski R.I., 1987, *MNRAS*, 226, 747  
 Jerjen H., Binggeli B., 1997, in *The Nature of Elliptical Galaxies*, ASP Conf. Series, Vol. 116, ed. M. Arnaboldi, G.S. Da Costa and P. Saha, p.239  
 Kormendy J., 1985, *ApJ*, 295, 73  
 Mateo M., Olszewski E., Welch D.L., Fischer P., Kunkel W., 1991, *AJ*, 102, 914  
 Moore B., Lake G., Katz N., 1998, *ApJ*, 495, 139  
 Paturel G., Fouqué P., Bottinelli L., Gouguenheim L., 1989, *A&AS*, 80, 299  
 Pedraz S., 2002, Ph.D. thesis, Universidad Complutense de Madrid, in preparation  
 Ryden B.S., Terndrup D.M., 1994, *ApJ*, 425, 43  
 Ryden B.S., Terndrup D.M., Pogge R.W., Lauer T.R., 1999, *ApJ*, 517, 650  
 Sargent W.L.W., Schechter P.L., Boksenberg A., Shortridge K., 1977, *ApJ*, 212, 326  
 Simien F., Prugniel P., 1997, *A&AS*, 126, 15  
 Smith R.J., Lucey J.R., Hudson M.J., Schlegel D.J., Davies R.L., 2000, *MNRAS*, 313, 469  
 Worthey G., Faber S.M., González J.J., Burstein D., 1994, *ApJS*, 94, 687

This paper has been typeset from a  $\text{\TeX}$ / $\text{\LaTeX}$  file prepared by the author.